6. Fluorescence Measurement

Principles and Techniques

Pedro Alberto da Silva Jorge
INESC TEC

Handbook of Optical Sensors. Edited by José Luís Santos and Faramarz Farahi © 2015 CRC Press/Taylor & Francis Group, LLC. ISBN: 9781439866856.

6.1 Introduction

Luminescence phenomena happen whenever an electronically excited species is deactivated by emission of ultraviolet (UV), visible, or infrared radiation. Depending on how the material is excited in the first place, the luminescent event can fit into different categories. If high-energy photons, from UV to blue, are the source of excitation, the emission is called photoluminescence; conversely, chemiluminescence happens when the excitation mechanism is a chemical reaction. A source of curiosity and fascination when observed in nature in earlier times (radioluminescence of aurora borealis, bioluminescence of fireflies), presently, luminescent phenomena are well understood and the basis for some of the most powerful analytical methods, providing the highest sensitivity. In this regard, photoluminescence is, by far, the most widely studied technique routinely applied in many well-established imaging and sensing methods (Lakowicz 1999, Kuhn and Forsterling 2000, Valeur 2002, Orellana 2004).

Traditionally, fluorescence-based analytical methods were associated with high-cost bulky laboratory equipment. However, a diversity of technological advances taking place over the last 20 years concurred to change this picture. In the field of optoelectronics, the advent of low-cost blue and UV lasers and LEDs, together with new miniature CCD spectrometers and high-sensitivity avalanche photodiodes (APDs), is enabling a new generation of spectroscopy tools to be developed and deployed in field applications. On the other hand, chemistry and material sciences are delivering new types of fluorescent materials with enhanced sensing properties, such as long-lived metallo-organic complexes or highly photostable quantum dots (QDs). Such developments are expanding the uses of fluorescence and enabling new applications such as long-term multiwavelength imaging, flow cytometry analysis in microfluidic chips, high-throughput DNA sequencing, and fiber-optic-based diagnostic probes.

In this chapter, the fundamental principles of photoluminescence spectroscopy and associated detection techniques will be presented. Standard methods and future trends of fluorescence-based sensing technologies and its applications will be discussed.

6.2 Principles of Photoluminescence

Photoluminescence phenomena take place in a spectral band ranging roughly from 200 to 1000 nm. Following the absorption of a photon, a molecule in an electronic excited state arises having available a diversity of decay mechanisms by which it can return to its fundamental state. In addition to photon emission, there are nonradiative decay routes in which energy is released in the form of heat. Alternatively, interaction with other molecules can result in nonemissive quenching processes. In some cases, the excited

molecule can undergo a chemical reaction losing its ability to fluoresce (photodegradation). Typically, following the excitation of a population of fluorescent molecules, all these processes can take place simultaneously, and whatever is observed depends on the relative probabilities and time scales of each phenomena. These processes depend on environmental conditions (temperature, relative concentrations, type of molecules, intensity of excitation, etc.). From the observed behavior, a wealth of information can be retrieved about a molecular system making photoluminescence a powerful analytical tool.

6.2.1 Fluorescence and Phosphorescence

Depending on the spin multiplicities of the ground and excited states involved, photoluminescence phenomena can be classified as fluorescence or phosphorescence. Fluorescent transitions usually take place between the excited singlet state of lowest energy and the ground singlet state; therefore, the electron gets to keep its spin in the transition. These are spin-allowed transitions characterized by high transition rates and lifetimes in the nanosecond range. Phosphorescence, on the other hand, results from transitions involving levels with electrons having the same spin orientation, called triplet states. Electrons have to change their spin during the transition. These are quantum mechanically forbidden transitions, with very small but nonzero probability of occurrence, resulting in low transition rates and much slower time scales (ranging from few microseconds to several milliseconds or even longer). The border, in the time domain, between these two processes is ill-defined but can be roughly set around 1 μs.

6.2.2 Molecular Orbitals

The absorption and emission of radiation observed in most luminescent dyes result from transitions between different energy levels, involving molecular orbitals. Depending on the shape of the initial atomic orbitals and on the degree of overlap, different kinds of molecular orbitals arise. Sigma (σ) bonds are the strongest type of covalent bonds resulting from strongly overlapping *s* or *p* atomic orbitals. Weaker overlap of *p* orbitals results in weaker bonding orbitals. These bonds are formed by π orbitals and usually arise in molecules having multiple bonds. In formaldehyde (H_2CO), for example, the double bond between carbon and oxygen is formed by a π and a σ orbital. The structural formula of formaldehyde is depicted in Figure 6.1 where the bonds are indicated. Due to the

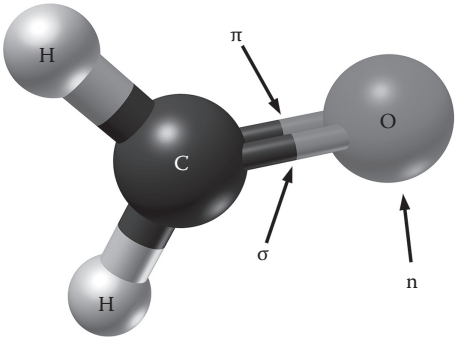

FIGURE 6.1 Structural formula of formaldehyde indicating different types of molecular orbitals.

presence of heteroatoms like oxygen and nitrogen, dye molecules can also have electrons that do not contribute to bonding. The corresponding molecular orbitals are called *n* orbitals and are also represented in the figure.

The promotion of electrons in π orbitals to antibonding orbitals, designated π*, can be achieved by absorption of photons with appropriate energy. The same is true for σ orbitals. Transitions between nonbonding *n* orbitals and antibonding orbitals are also possible. The transitions $\pi \rightarrow \pi^*$ and $n \rightarrow \pi^*$ occur by absorption of UV and visible photons (in the 200–700 nm region) and are the most relevant to fluorescence phenomena.

Considering a molecule in the fundamental state, the highest occupied molecular orbital (HOMO) and the lowest unoccupied molecular orbital (LUMO) are particularly important for spectroscopy applications. The difference in energy between these two orbital corresponds to the minimum necessary to optically excite the molecule and establishes the onset of absorption. In formaldehyde, the HOMO is an *n* orbital and the LUMO is a π* orbital.

In molecules like formaldehyde with a single double bound, the orbitals are localized between pairs of atoms, confining the electronic wave function. In longer molecules, however, where double and single carbon–carbon bonds alternate, the overlap of different π orbitals allows for electrons to spread over the whole molecule. The reduced confinement of the electronic wave function results in lower energies for the $\pi \rightarrow \pi^*$ transitions and in a corresponding shift of the absorption to longer wavelengths. This way, the absorption and emission properties of molecular dyes are strongly dependent on the molecular structure and will be defined by the orbitals arrangements. This provides a mechanism for chemical engineers to control the luminescent properties of dyes, which can be tailored for a specific application (Kuhn and Forsterling 2000).

6.2.3 Nonradiative Processes

Besides photon emission, there are many possible mechanisms through which an excited molecule can return to the fundamental state. Intrinsic processes include internal conversion (nonemissive vibrational relaxation), intersystem crossing (conversion from singlet to triplet states, with higher probability of nonradiative deactivation), intramolecular charge transfer, and conformational changes. Extrinsic processes, on the other hand, involve interaction of the excited luminophores with other molecules. Through these interactions, the excited states can be quenched by electron transfer, proton transfer, energy transfer, or excimer formation.

Whether the absorption of a photon ultimately results in the emission of a photon or in some other energy transfer will depend on the relative time scales of all the processes involved (Table 6.1). For instance, long-lived phosphorescence is seldom observed in solutions because, at ambient temperature, many faster processes (relaxation and quenching) compete for deactivation. Fluorescence, on the other hand, being much faster than many nonradiative processes is easily observed. This way, the emission properties of most luminescent dyes is highly sensitive to the microenvironment surrounding the excited molecule. Factors like temperature, pH level, pressure, presence of ions, and polarity can strongly impact the luminescence output. Many of the luminescence parameters, like quantum yield, lifetime, and spectral distribution, can thus be used to probe the environment with extreme sensitivity, providing

Table 6.1 Characteristic Time Scales of the Different Radiative and Nonradiative Transitions Involved in Luminescence Processes

Transition	Characteristic Times (s)
Absorption	10^{-15}
Vibrational relaxation	10^{-12}–10^{-10}
S_1 excited state lifetime	10^{-10}–10^{-7} fluorescence
Intersystem crossing	10^{-10}–10^{-8}
Internal conversion	10^{-11}–10^{-9}
T_1 excited state lifetime	10^{-6}–1 phosphorescence

Source: Data from Valeur, B., *Molecular Fluorescence: Principles and Applications*, Wiley VCH, Weinheim, Germany, 2002.

both spatial and temporal information. Depending on the lifetime of the molecular probes, dynamic processes with different time scales can be monitored (e.g., diffusion, chemical reactions, biological process). The high sensitivity and specificity (different molecular probes have different susceptibilities) of luminescence to environment parameters explain its success as an analytical tool and provide the basis for its application in optical sensing (Wolfbeis 1997).

Usually, the spectroscopic properties of a molecule are determined by the intramolecular processes. The effect of the external intermolecular processes over these properties can then be used as a probe of the molecular environment.

6.2.4 Absorption and Emission Spectra

The absorption and emission spectra of a molecular dye are primarily established by the possible electronic transitions. In addition, a set of vibrational sublevels, of much lower energy, is associated to each electronic state, multiplying the number of possible transitions.

The study of the processes that determine the spectral distribution of absorption and luminescent emission is usually performed using Perrin–Jablonski diagrams (Lakowicz 1999). In Figure 6.2a, an example of such diagram is represented, showing the radiative and nonradiative transitions involved in luminescent processes. External mechanisms, like quenching by other molecules, are not shown. The singlet (S) and triplet states (T) are represented by thick horizontal lines. The thin horizontal lines represent the vibrational levels associated with each electronic state.

At room temperature, most electrons are in the lowest vibrational level of the fundamental state following a Boltzmann distribution. Higher energy electronic levels can be populated by absorption of visible or UV radiation. Depending on the photons energy, electrons in the ground level can be promoted to different vibrational levels of the excited singlet states (S_1 or S_2). In the timescale of the absorption process (10^{-15} s), nuclear displacement can be neglected, so electronic transitions tend to occur between vibrational levels having identical nuclear configuration in both states (Franck–Condon principle). As a consequence, electrons are usually promoted to higher vibrational levels of the electronic excited state. As the nuclear configuration accommodates and releases the excess energy, electrons rapidly relax to the lowest vibrational level of S_1.

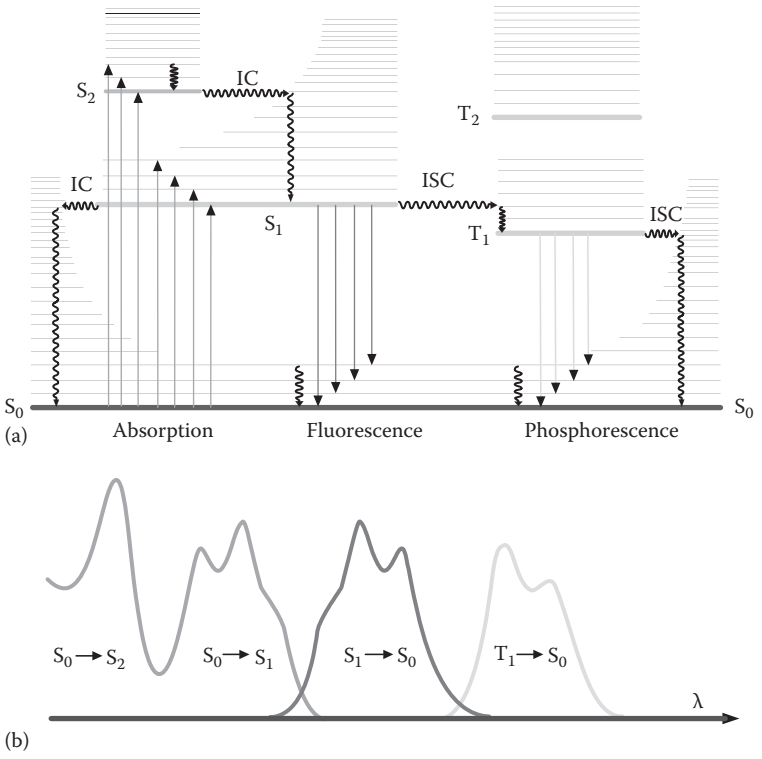

FIGURE 6.2 (a) The Perrin–Jablonski diagram illustrating the different transitions involved in luminescent processes. IC, internal conversion; ISC, intersystem crossing. Straight arrows represent radiative transitions and curly arrows nonradiative processes. (b) Corresponding absorption and emission spectra. (Adapted from Valeur, B., *Molecular Fluorescence: Principles and Applications*, Wiley VCH, Weinheim, Germany, 2002.)

The structure of the molecular absorption spectrum will therefore reflect the structure of the excited vibrational levels. The relative strength of each vibrational absorption line will depend on the molecular configuration and is proportional to the overlap of the wave functions of the two states involved in the transition. In Figure 6.2b, the absorption spectrum that results from the transitions represented in the respective Jablonski diagram is shown. In the band corresponding to the $S_0 \rightarrow S_1$ transition, different vibrational peaks can be identified. Due to inhomogeneous broadening, the vibrational structure is smoothed and can sometimes become unnoticeable.

Because internal conversion processes are usually faster than the fluorescence lifetimes, emission tends to occur from the lowest vibrational level of the excited state. This way, the energy of the emitted photons is always smaller than the energy of the absorbed photons. The wavelength difference between the absorption and emission peaks is called the Stokes shift and enables the spectral discrimination of the excitation and emission radiations. In practice, its value will determine the filtering and signal processing requirements of the instrumentation.

The return to the ground state usually occurs to excited vibrational levels. Further vibrational relaxation will then restore the system in thermal equilibrium placing almost all the electrons in the fundamental state. This way, the vibrational level structure,

which depends mostly on the nuclear configuration, can also be seen in the emission spectrum. In fact, the emission spectrum is usually a mirror image of the absorption spectrum (see Figure 6.2b and corresponding transitions in the diagram of Figure 6.2a). The same homogeneous and inhomogeneous broadening processes that affect absorption will also impact the resulting emissions spectrum. This way, molecular dyes usually present relatively broad emission spectra.

Through intersystem crossing, an electron in the short-lived excited singlet level, S_1, can have its spin inverted being transferred to a long-lived excited triplet state, T_1. Radiative transition rates of molecules in excited triplet states correspond to phosphorescence and are orders of magnitude smaller than those of fluorescence. Because triplet states are of lower energy, phosphorescence occurs at longer wavelengths. Their longer radiative lifetimes favor nonradiative return to the ground state, through vibrational relaxation. These processes are particularly favored in solutions and at ambient temperature due to collisions with solvent molecules. In these conditions, radiative quantum yields are usually very low and phosphorescence is seldom observed. Conversely, at low temperatures or in solid state, phosphorescence can be detected, showing greatly increased lifetimes (ms to min). In addition, in molecules containing heavy atoms, there is higher spin–orbit coupling and intersystem crossing is favored increasing phosphorescence quantum yields.

The luminescence emission spectrum observed is usually independent of the wavelength of the excitation radiation. This happens because, even when the absorbed energy exceeds that of the HOMO/LUMO gap, due to the fast relaxation processes, electrons always end up in the lowest vibrational levels of S_1 or T_1. This way, the intensity of the luminescent signal observed, at a fixed wavelength, is proportional to the excitation power and to the absorbance at that particular wavelength. The plot of the luminescent intensity as a function of the incident wavelength is called excitation spectrum. If corrections are made to compensate for variation of the excitation source spectral distribution, the excitation spectrum will coincide with the absorption spectrum.

6.2.5 Excited State Lifetime

After excitation, not all molecules emit precisely at the same instant. Spontaneous emission is a random process with all molecules having identical emission probability in a certain interval. The average time a molecule stays in the excited state before returning to the fundamental state is called the fluorescence lifetime, τ_0, and it depends on the rate constants associated with all the radiative and nonradiative mechanisms involved:

$$\tau_0 = \frac{1}{k_r^S + k_{nr}^S} \tag{6.1}$$

In this relation, k_r^S stands for the radiative rate constant of fluorescence, associated with the $S_1 \rightarrow S_0$ transition. k_{nr}^S, on the other hand, results from adding the nonradiative rates associated with the processes of internal conversion, k_{IC}^S, and intersystem crossing, k_{ISC}^S.

This way, when a fluorescent sample is excited by a δ-like pulse of light, a given concentration of excited molecules is initially obtained that decreases at a rate of $1/\tau_0$. Because the intensity of the luminescent signal, I, is proportional to the concentration of excited molecules, following a pulsed excitation, the output luminescence intensity decreases in an exponential fashion with a time constant given by τ_0:

$$I(t) = I_0 e^{-t/\tau_0} \tag{6.2}$$

where I_0 is the luminescence intensity, immediately after excitation. This way, in practice, τ_0 can be defined as the time it takes for the fluorescence intensity to decrease by $1/e$ of its initial value. The function $I(t)$ is the impulse response of the system. The response of the luminescence output to complex excitation patterns can be obtained by convolution of this function with the exciting impulse. In the case where intersystem crossing is favored, phosphorescence will be obtained instead. Similar expressions can be obtained using the corresponding rate constants.

6.2.6 Quantum Yield

The quantum yield of a luminescent dye is a measure of its efficiency and can also be estimated from its rate constants. It is defined as the ratio between the number of emitted photons by the number of absorbed photons and it can be calculated from

$$\Phi = \frac{k_r}{k_r + k_{nr}} \tag{6.3}$$

The quantum yield depends on the relative magnitudes of the radiative and nonradiative rate constants, and it will always be less than unit, on account of the Stokes shift. In practice, the value of Φ results from the summation of all the photons emitted during the decay interval divided by the number of absorbed photons. Considering the same excitation optical power, the higher the quantum yield, the easier it will be to detect the luminescent signal of a given sample.

The lifetime and the quantum yield are two fundamental parameters of luminescent emission. They determine the intensity of the luminescent signal and its temporal behavior. In addition to the intrinsic deactivation mechanisms described earlier, the interaction with other molecular species introduces further nonradiative decay routes that can have a strong impact in both these parameters. The monitoring of the lifetime and/or quantum yield, under the influence of such mechanisms, provides the basis for very sensitive sensing techniques.

6.3 Fluorescence Measurement Techniques

In order to implement a practical fluorescence spectroscopy system, measurements of the luminescent properties must be performed. Luminescence detection techniques can be broadly classified into two main types of measurements, steady-state and time-resolved measurements (Valeur 2002).

6.3.1 Intensity-Based Spectroscopy

In steady-state spectroscopy, the luminescence spectra or the luminescence intensity are recorded while submitting the sample to continuous illumination with an adequate excitation source. Although simple in principle, the measurement of luminescence intensity can be a complex task as it depends on a great deal of intrinsic properties as well as experimental parameters.

6.3.1.1 Absorbance

An efficient excitation depends on the spectral overlap of the exciting radiation with the dye absorption spectrum. The absorption efficiency depends on the intrinsic properties of the fluorescent dye as well as on practical experimental parameters. Macroscopically, the absorption efficiency can be evaluated by the absorbance of a sample:

$$A(\lambda) = \log \frac{I_0(\lambda)}{I_T(\lambda)} \tag{6.4}$$

where $I_0(\lambda)$ and $I_T(\lambda)$ are the excitation light intensities entering and leaving the absorbing medium, respectively (excluding the luminescent emission).

The absorbance is proportional to the dye concentration, c, the sample thickness, l, and the molar absorptivity, ε, following the Beer–Lambert law:

$$A(\lambda) = \varepsilon(\lambda) l c \tag{6.5}$$

The molar absorptivity is an intrinsic parameter determined by quantum mechanical factors defining the strength of absorption at each particular wavelength.

According to the Beer–Lambert law, the sample absorbance increases linearly with increasing dye concentration. This way, the more concentrated or thicker the sample, the more efficient will be the excitation process. However, for very high concentrations, deviations from linearity are often observed. This may be due to saturation effects leading to the formation of dye aggregates, which scatter light or may have modified absorption. Sample turbidity and light scattering can also impact the measured absorbance. The accurate application of the Beer–Lambert law, in an experimental situation, must also take into account the reflections at the sample interfaces, detection solid angle, etc. In practice, it is not straightforward to determine the optical power actually reaching the sample or the luminescent power actually leaving the sample. Absorbance also increases with the sample thickness; however, for practical reasons, l cannot be made too large. All these factors should be carefully considered when preparing a luminescent sample.

6.3.1.2 Steady-State Luminescence

Considering a luminescent sample under continuous illumination, equilibrium is usually achieved between the excitation and the deactivation mechanisms, and the concentration of excited luminophores remains constant. This means that the excited state population attains a steady state. It can be shown that in such situation, in addition to

the dependence on the excitation efficiency, the luminescent output will depend also on the quantum yield:

$$I_L = I_0\left(1-10^{-\varepsilon cl}\right)\Phi \tag{6.6}$$

The quantum yield is an intrinsic parameter of the luminescent material, proportional to the relative magnitudes of the radiative and nonradiative decay rates. This way, for obtaining a strong luminescence output, materials with high quantum yields should be chosen. Although a smaller quantum yield could be compensated by increasing the excitation intensity, this is not a desirable situation as it will also increase photodegradation processes.

6.3.1.3 Emission Spectrum

In practice, the photons emitted follow a certain energy distribution, $F(\lambda_L)$, which defines the characteristic emission spectrum of a given luminophore. Experimentally, such distribution together with the associated Stokes shift will determine the characteristics of the necessary detection instrumentation (filtering, detector spectral range, etc.).

Ultimately, the detected luminescent intensity, I_L, will depend on the incident excitation intensity $I_0(\lambda_{Ex})$, the absorption and emission spectral features of the luminophore, and the particular experimental arrangement:

$$I_L\left(\lambda_{Ex},\lambda_L\right) = 2.3kF\left(\lambda_L\right)I_0\left(\lambda_{Ex}\right)\varepsilon\left(\lambda_{Ex}\right)lc \tag{6.7}$$

The parameter k accounts for a diversity of experimental factors affecting the detected signal (detection geometry, wavelength dependence of detector sensitivity, system spectral resolution, polarization effects, filtering, electronic gain, etc.), some of which can hardly be quantified. This way, the numerical value of a luminescence intensity measurement has no direct physical meaning and is usually expressed in arbitrary units or simply normalized to a reference value.

This equation also demonstrates that the detected luminescent signal depends on a great number of intrinsic and experimental parameters, which should be considered thoroughly for an accurate interpretation of the obtained data. Conversely, it also provides a good insight into the many ways the signal detection, and thus a luminescent sensor sensitivity, can be optimized.

Equation 6.7 is an approximation for low luminophore concentrations and deviations from linearity can be observed with increasing absorbance. Inner filter effects, due to self-absorption of attenuation of excitation in thick samples, may take place that reduce the observed signal. The presence of impurities providing scattering centers or background luminescence can further complicate the observed behavior.

When I_L is measured as a function of λ_L, for a fixed excitation wavelength, λ_{Ex}, the emission spectrum is obtained (i.e., a signal proportional to $F(\lambda_L)$). On the other hand, if the luminescent intensity is measured at a fixed wavelength, λ_L, while changing the excitation wavelength, λ_{Ex}, the excitation spectrum can be obtained instead (i.e., a signal proportional to $A(\lambda_{Ex})$).

6.3.1.4 Instrumentation

Spectral measurements of fluorescent intensity are usually performed using a spectrofluorometer. These instruments usually consist in a broadband optical source, followed by a monochromator to select the excitation wavelength. The selected radiation is then shined upon the luminescent sample and detection is usually made at 90° with the incident beam. In order to perform wavelength discrimination of the luminescence emission, a second monochromator is placed before the detector, usually a photomultiplier. An ideal spectrofluorometer would have an optical source with a constant photon output at all wavelengths ($I_0(\lambda_{Ex})$ = const.), monochromators with polarization and wavelength independent efficiency, and a detector with equal sensitivity at all wavelengths. Unfortunately, such ideal components are not available and, in practice, corrections must be performed in order to account for these imperfections.

Instrumentation used in practice introduces a series of wavelength dependencies that cause distortion of the measured spectra if no corrective measures are taken (Lakowicz 1999). High-pressure xenon arc lamps are widely used as excitation sources. Except for a few sharp lines near 450 and 800 nm, these lamps provide a relatively continuous light output in a broad wavelength range (250–700 nm), which can be used to excite most luminophores. Selection of the excitation wavelength using a monochromator results in low optical power reaching the sample. It is possible to use other lamps that provide higher intensities in the UV region, like mercury lamps or mercury–xenon lamps. In these cases, however, the optical power is further concentrated in sharp spectral lines.

The monochromators also have a wavelength-dependent efficiency. This dependence arises mostly from their dispersive element, typically a diffraction grating, which usually has maximum diffraction efficiency at a given wavelength. Also, scattering and higher-order diffraction can increase the levels of stray light reaching the detector and further distort the measured spectra. On top of this, the efficiency of monochromators is typically dependent on the polarization of the incident radiation. This can be a problem because the luminescent emission is often anisotropic and can be partially polarized (Valeur 2002). In order to avoid polarization dependence, usually the excitation radiation is linearly polarized, and detection is performed through a second polarizer at 54.7° with the input polarization (called magic angle). In these conditions, it can be demonstrated that the signal detected is always proportional to the total luminescent intensity.

Typically, photomultiplier tubes are used for detection in steady-state measurements due to their high sensitivity. More recently, linear and 2D CCD detectors are also being used in many devices and practical applications. Unfortunately, all these detectors have a wavelength-dependent sensitivity that must be accounted for.

Due to the wavelength dependence of the optical source, most of the time, the only way to obtain accurate spectral measurements is to provide for a reference channel. For this purpose, in spectrofluorometers, a few percent of the excitation radiation is usually deviated toward a second detection channel. Generally, this light is detected by a photodiode with an approximately spectrally flat response. In alternative, a quantum counter is used. A quantum counter usually consists in a concentrated solution of a dye with a quantum yield that does not depend on λ_E. This way, all the incident photons are absorbed and the emitted luminescent signal detected by

the reference detector is proportional to the photon flux incident in the sample under study. In principle, ratiometric detection of the signal from the main detector with the signal from the reference detector will allow compensation of the wavelength dependences of the excitation optical source, excitation monochromator efficiency, and detector sensitivity. In addition, fluctuations of the excitation source output intensity over time will be compensated as well.

Most of the time, however, because the optical path of both channels is not exactly the same, full compensation cannot be achieved. In addition, with this method, the detection monochromator is not accounted for. In cases where very accurate measurements are needed, usually a standard dye is used with known emission and excitation spectra. The spectra of this dye are then measured and compared with the expected spectra, allowing the calculation of adequate correction factors. Alternatively, instrument correction factors can also be obtained by measuring the spectrum of a calibrated light source transmitted through a transparent scattering solution. The determination of quantum yields is an example of a measurement only possible using accurately corrected spectra. For this particular application, the use of standard dyes, with known quantum yield, must be considered for accurate calibration of the system.

Whenever it is adequate to measure fluorescence intensity at a single excitation and emission wavelength, filter-based spectrometers can be used instead. The use of filters to select wavelength allows much higher excitation and luminescence collection efficiencies. Therefore, filter-based instruments are often used in ultratrace analysis, where it is crucial to maximize the fluorescence signal at the expense of selectivity. This approach is often used in low-cost portable analytical instruments and in a variety of luminescence-based sensors targeting specific analytes.

In summary, the main difficulty associated with intensity-based measurements arises from the fact that the detected intensity is not an intrinsic parameter of the luminescent dye. It depends on intrinsic properties of the luminophore, like the quantum yield, but also on a great diversity of external parameters. The control of all this variables is critical when aiming to obtain accurate information on the dye intrinsic properties like quantum yields and emission and absorption spectra. Nevertheless, whenever the quantification of an analyte is at stake, simpler configurations can be explored for low-cost high-sensitivity detection.

6.3.2 Time-Domain Spectroscopy

Time-resolved measurements of the luminescence intensity are a powerful alternative to steady-state measurements (Lakowicz 1999, Valeur 2002). Lifetime is an intrinsic characteristic of the luminophore; therefore, measurements are not so susceptible to system changes such as optical alignment, dye concentration, or even photodegradation.

The observation of luminescent decay, which occurs in very short time scales, provides the opportunity to monitor many transient behaviors of molecular systems, which may become unnoticeable under steady-state excitation. In general, the study of the dynamics of excited states provides much more information about the system being studied than is possible to achieve with steady-state data. These techniques therefore have a fundamental role in the study of the kinetics of many photophysical, photochemical, and photobiological processes.

Time-resolved measurements can be made in the time domain or in the frequency domain. The two methods are widely used nowadays both in laboratorial environment and in sensing applications. Time-domain methods will be described first.

6.3.2.1 Pulse Fluorometry

The basic principle of time-domain techniques is the excitation of the sample with a short pulse of light and the observation of the subsequent luminescent decay. The pulse width should be made as short as possible, preferably much shorter than the lifetime of the dye under study.

In the simplest case, the luminescent sample response, $I(t)$, to a δ-pulse excitation, is single exponential with a time constant equal to the excited state lifetime (Equation 6.2). A simulation of the data obtained in this ideal situation is represented in the diagrams of Figure 6.3. If the intensity is measured as a function of time, the decay time can then be estimated from the slope of the linear plot of $\log I(t)$ (Figure 6.3b) or from the time at which the intensity drops to $1/e$ of its initial maximum value at $t = 0$ (Figure 6.3a).

In practice, however, the excitation pulse has a short but finite time width, not negligible in comparison with the lifetime to be measured. In addition, the response time of the detection system can introduce further broadening in the measured signals. In such cases, the luminescent response will be given by the convolution of the ideal δ-pulse response, $I(t)$, with a function, $E(t)$, describing the real excitation impulse as perceived by the detection system:

$$R(t) = E(t) \otimes I(t) = \int_{-\infty}^{t} E(t')I\left(t - t'\right)dt' \tag{6.8}$$

In order to obtain the lifetime of the luminophore from the measured data, the impulse response of the excitation/detection system ($E(t)$) must be known very accurately, and a deconvolution must be performed. Much of the complexity of lifetime data analysis comes from the difficulty in extracting the true luminophore δ-impulse response

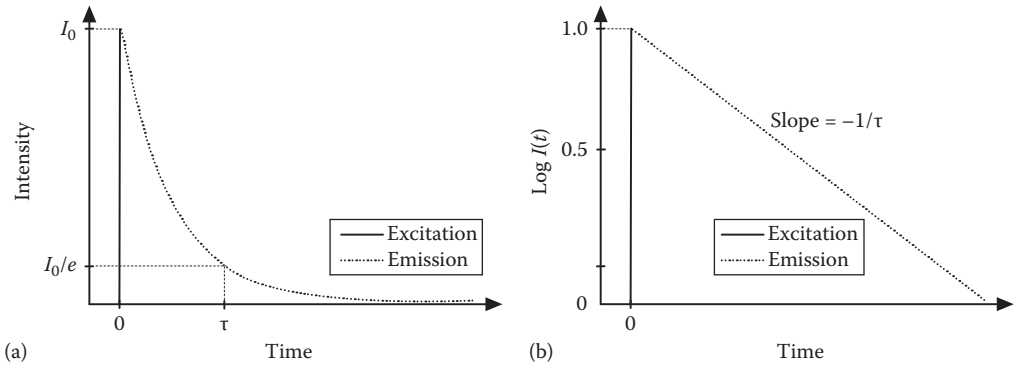

FIGURE 6.3 Principles of time-resolved measurements. (a) After an impulse excitation, luminescent intensity decays exponentially with a time constant given by the lifetime. (b) The decay time can be calculated from the slope of $\log I(t)$. (Adapted from Lakowicz, J.R., in *Principles of Fluorescence Spectroscopy*, 2nd Edition, Kluwer Academic/Plenum Publishers, New York, pp. 96, 1999.)

from the measured signals. For this reason, a great effort is placed in the optimization of the deconvolution process. Nevertheless, interpretation of data arising from single-exponential decays is relatively straightforward. The real challenge comes from the fact that most samples display more than one decay time.

6.3.2.2 Multiple-Exponential Decays

Multiple lifetimes can arise from the presence of different luminescent species in the same sample or from a single dye in a heterogeneous environment. In such case, different lifetimes may be assigned to each population. In general, complex decay functions can be fitted by a multiexponential model described by

$$I(t) = \sum_i \alpha_i e^{(-t/\tau_i)} \tag{6.9}$$

where

α_i are called the pre-exponential factors and determine the amplitudes of each component at $t = 0$

τ_i are the respective lifetimes

Depending on the system being studied, the meaning of these parameters may differ. For a single dye existing in different environments, usually both populations have the same radiative decay rate, in such case α_i represents the relative fraction of each luminophore. For a mixture of different luminescent species, however, the relative values of α_i depend on many parameters, like the quantum yield and relative concentration. In these cases, assigning a molecular meaning to each α_i is not straightforward. Nevertheless, it is always possible to estimate the fractional contribution of each species.

The simplest case to consider is the presence of two different populations. Usually, the presence of a second lifetime will introduce a curvature in the plot of log$I(t)$. Fitting the obtained data with Equation 6.9 will then allow recovering the decay parameters. However, depending on the relative magnitudes of the different parameters, the change in the decay data can be very small, may be present only in the end of the decay tail, and sometimes is barely noticeable by simple observation. For this reason, it is important to capture the whole decay function, which demands for a high signal-to-noise ratio. As the number of fractional contributions increases, the interpretation of data becomes increasingly complex, and to extract the values of α_i and τ_i, from the observed decay measurements, is not a trivial task. This happens because the parameters α_i and τ_i are correlated, meaning that the same decay data may fit different combinations of α_i and τ_i. In practice, it is not possible to resolve two lifetimes if they differ from less than 20%.

For these reasons, evaluation of the fitting quality is a critical step of lifetime measurements and is usually done with the help of dedicated software. Many models have been explored to evaluate the quality of fitting: methods of least squares, moments, Fourier transforms, Laplace transforms, and others. The most widely used method is based in nonlinear least squares where the basic principle is to minimize a correlation parameter, χ^2, that represents the mismatch between the theoretical model and the experimental data.

Although mathematical tools provide valuable help, careful analysis and a lot of experience is necessary for accurate interpretation of lifetime data.

Regardless of the number of exponential terms considered, it is always possible to define an average or apparent decay time, $\langle\tau\rangle$. Such average parameters are of particular interest for sensing applications where, for instance, the analyte concentration can be derived from the apparent lifetime. In this context, analysis of lifetime data can be greatly simplified.

6.3.2.3 Techniques and Instrumentation

There are many ways to record lifetime data, such as streak cameras and boxcar integrators. Nevertheless, most instruments used for the determination of lifetimes are based in the time-correlated single-photon counting (TCSPC) method, also called as single-photon timing (SPT). This technique is based on the fact that the probability of detecting a single photon at the time t after excitation is proportional to the luminescence intensity at that time. This way, measuring the time between the excitation pulse and the first arriving photon, at different times and for a large number of excitation impulses, it is possible to reconstruct the intensity decay curve, based on the obtained histogram of photon counts per time channel. Because only a single photon is detected by measurement cycle, this technique requires a large number of measurements in order to completely reconstruct the decay function. SPT can be very sensitive but, although conceptually simple, it is associated with complex instrumentation, which, ultimately, will determine the sensitivity and time resolution that can be achieved.

The excitation source is of primary importance and it should provide narrow pulses with a relatively high repetition rate. Initially, excitation was provided mainly by flash lamps, which delivered low-intensity *ns* pulses with repetition rates in the 10–100 kHz range in a limited spectral range (200–400 nm). Flash lamps are relatively inexpensive, and by using deconvolution, it is possible to measure lifetimes in the hundreds of picoseconds range. However, low repetition rates demand for long acquisition times where lamp drift can become a problem. Nowadays, although more expensive, lasers are used as the preferred excitation source. A mode-locked laser associated with a dye laser or Ti–sapphire laser can easily provide picoseconds pulses, at high repetition rates (MHz) and in a wide range of wavelengths. More recently, *ps* systems based in laser diodes are becoming available at a variety of wavelengths.

The time resolution of the instrument is also critically determined by the sampling and detection electronics. While standard dynode chain photomultiplier tubes (PMT) can provide response times in the *ns* range, nowadays, microchannel plate (MCT) PMTs are available capable of operating 10–20 times faster. Nevertheless, this new generation of PMTs is considerably more expensive. Although photodiodes are much cheaper and can respond faster than MCT PMTs, they lack sensitivity. APDs have adequate gain, but their fast response is dependent on a very small size active area (10 × 10 μm). This way, APDs do not have the necessary sensitivity for most measurements. With mode-locked lasers and MCT photomultipliers, widths of the instrument pulse response in the range 30–40 ps can be achieved. This allows the measurement of decay times as short as 10–20 ps.

Although source and detector are the key elements in lifetime measurements, these techniques rely also on a variety of sophisticated electronic devices like synchronization electronics, time-to-amplitude converters, filtering, and delays lines, which add to

the cost and complexity of the measurement system. In addition, several problems in data collection can arise that must be considered like polarization effects, scattering in turbid solutions, and wavelength dependence of the measurement system. Solving these problems often demands for additional data processing, use of filtering, or even using a reference channel.

Generally, the shorter the lifetime, the more expensive and complex the measurement system becomes. This way, the use of standard organic fluorophores, with lifetimes in the nanosecond range, can be a serious obstacle to the implementation of low-cost sensing applications using time-resolved detection techniques. In this regard, the advent of long-lived luminescent probes, like organometallic complexes, can provide interesting solutions. Because these sensing dyes present lifetimes in the microsecond range, the instrumentation can be greatly simplified. In these time scales, system impulse responses of tens of nanoseconds wide are acceptable, which can be achieved by diode lasers or even low-cost LEDs in combination with photodiodes.

6.3.3 Frequency-Domain Spectroscopy

The measurement of excited state lifetimes can also be performed in the frequency domain, as an alternative to the time-domain techniques just described (Zhang et al. 1993, Lakowicz 1999).

6.3.3.1 Frequency-Domain or Phase Modulation Fluorometry

In frequency-domain spectroscopy, the excitation optical source is modulated in amplitude at high frequency. Typically, sinusoidal modulation is applied at frequencies that should be in the range of the reciprocal of the decay time. In these circumstances, the obtained luminescent emission is also modulated in amplitude at the same frequency. Due to the time lag between excitation and emission, however, the luminescent signal has a phase delay relative to the excitation. This way, the phase delay, ϕ, can be used to calculate the lifetime. The scheme in Figure 6.4 shows the typical

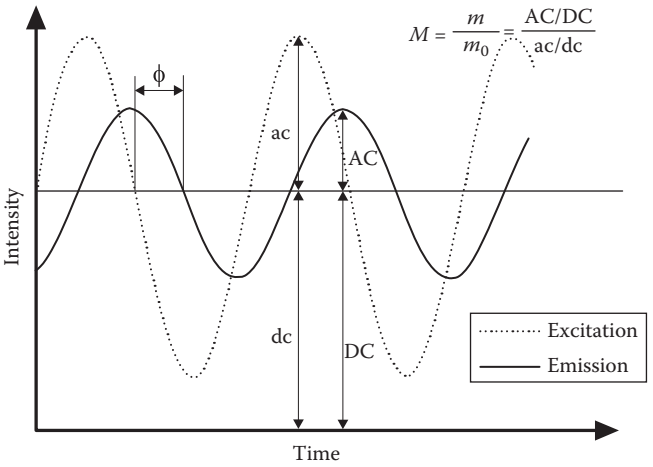

FIGURE 6.4 Response of luminescence emission to intensity-modulated excitation, showing the relative phase delay, ϕ, and modulation ratio, *M*.

response of a luminophore submitted to amplitude modulated excitation. This scheme also shows that, in addition to the phase delay, the resulting signal can present a decreased modulation depth, m = AC/DC, in comparison to the excitation signal, m_0 = ac/dc. The decrease in modulation depth is also called demodulation and it happens because the luminescent response is given by the convolution of the impulse response with the sinusoidal modulation. This way, for a fixed modulation frequency, the longer the decay tail of the luminophore impulse response, the greater the extent of the demodulation will be. Evaluation of the modulation ratio, $M = m/m_0$, can also be used to calculate the lifetime.

Typically, the relative phase, ϕ, and modulation ratio, M, are evaluated in a range of frequencies and the curves obtained characterize the harmonic response of the system. It is possible to demonstrate that the harmonic response corresponds to the Fourier transform of the δ-pulse response. This way, the two techniques are theoretically equivalent, in the sense that they analyze the same physical phenomenon although operating in different domains (time and frequency). However, they differ in the measurement methods and necessary instrumentation. When the data are evaluated directly in the frequency domain, no deconvolution is necessary.

6.3.3.2 Calculation of the Lifetime

In order to extract the decay information, from the frequency-domain data, it is necessary to relate ϕ and M with the lifetime τ. Assuming a single-exponential decay, the δ-impulse response of the luminophore can be described by Equation 6.2. In such case, the differential equation describing the time-dependent luminescent intensity is given by

$$\frac{dI(t)}{dt} = -\frac{1}{\tau} I(t) + E(t) \tag{6.10}$$

where $E(t)$ is the function describing the excitation radiation. In the particular case of sinusoidally modulated excitation, this function can be described by

$$E(t) = a + b \sin \omega t \tag{6.11}$$

where

ω is the angular modulation frequency
a and b correspond to the dc and ac components, respectively, of the incident intensity

This way, the modulation depth of the excitation function is given by $m_0 = a/b$. The luminescent dye will respond to this excitation with a luminescent output at the same frequency but shifted in phase and presenting a different modulation depth. Then, it can be assumed that the time-dependent luminescent intensity, $I_L(t)$, is described by a function like

$$I_L(t) = A + B \sin(\omega t - \phi) \tag{6.12}$$

When the sample is submitted to the sinusoidal excitation described by Equation 6.11, Equation 6.12 should be a solution to the differential equation (6.10). From the substitution of $I_L(t)$ and $E(t)$ into Equation 6.10, we can easily derive the following relations between the lifetime and the phase delay:

$$\tan \phi = \omega\tau = 2\pi f\tau \tag{6.13}$$

and the lifetime and the modulation ratio

$$M = \frac{B/A}{b/a} = \frac{1}{\sqrt{1+\omega^2\tau^2}} \tag{6.14}$$

This way, experimental measurements of the phase angle, ϕ, and the modulation ratio, M, can be used to calculate the lifetime.

6.3.3.3 Frequency-Domain Data

In practice, these parameters are usually evaluated in a range of frequencies, and the corresponding theoretical equations are then fitted to the measured data. A typical set of frequency-domain data was simulated using Equations 6.13 and 6.14, assuming a single-exponential decay with $\tau = 1.0$ μs. The results obtained are shown in Figure 6.5.

For lower modulation frequencies, the decay tail is negligible in comparison to the modulation period; this way, the emission closely follows the excitation, the phase delay is very small, and the relative modulation depth is nearly unit. However, as the modulation frequency approaches values near the reciprocal of the lifetime, the phase delay rapidly increases, and the modulation starts to fade. This is the frequency range where the rates $\partial\phi/\partial f$ and $\partial M/\partial f$ are higher and which contains more information about the sample parameters. The calculation of the optimal modulation frequency, where the phase has maximum sensitivity to lifetime changes, yields a frequency given by the reciprocal of

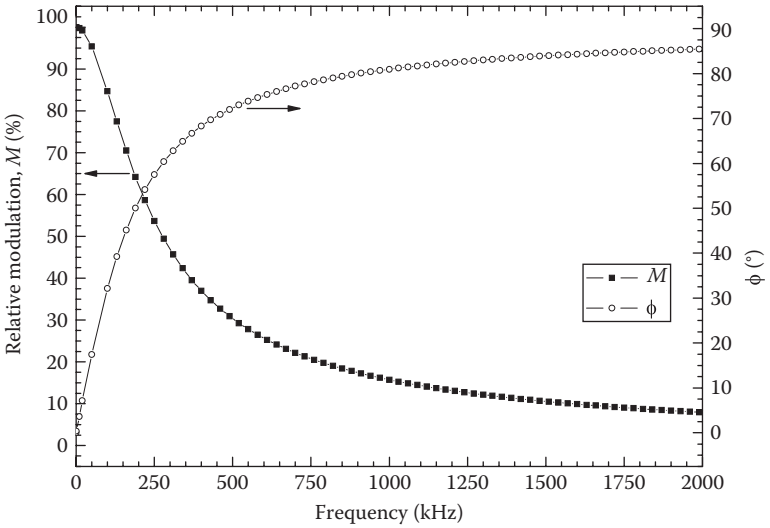

FIGURE 6.5 Simulated data showing relative phase, ϕ, and modulation ratio, M, as a function of the modulation frequency, for a single-exponential decay with $\tau = 1.0$ μs.

the luminophore lifetime ($f_{opt} = 1/2\pi\tau$). For higher frequencies, as the decay tail starts to overlap several modulation periods, the modulation depth decreases toward zero and the luminescent emission becomes continuous. Simultaneously, the phase delay grows very fast, and it converges asymptotically to 90° as the modulation vanishes. For samples with shorter lifetimes, the frequency range of interest (where the two curves cross) is shifted for higher frequencies.

This way, frequency-domain data provide two independent measures of the lifetime, which can be evaluated by measuring phase, τ_ϕ, or assessing the relative modulation, τ_M. If the decay is a single exponential, the values obtained with the two measurements should be the same, identical to the sample lifetime, and independent of the modulation frequency. In such cases, measurement can be performed at a single frequency and lifetime determination can be very fast.

6.3.3.4 Multiple-Exponential Decays

Most of the time, however, multiple-exponential decays are observed. In such cases, the two independent measures of the lifetime, τ_ϕ and τ_M, yield different values that are dependent of the modulation frequency, decreasing for higher frequencies. The measured values are just apparent and result from a complex weighting of various decay parameters. Although characteristic of the system under study, these are not true molecular parameters. Nevertheless, it can be useful to monitor the apparent lifetime, at a fixed frequency, using one of these techniques. Many sensing applications were reported, where the apparent lifetime was monitored in order to determine changes in the quencher concentration, using frequency-domain techniques.

In general, however, to fully characterize a complex decay, measurements should be performed in the widest possible frequency range, centered at a frequency near the reciprocal of the lifetime. The frequency-domain data for a multiexponential decay can be calculated from the sine and cosine transforms of the δ-impulse response $I(t)$. The experimental data obtained must be fitted to a theoretical curve. Judgment of the fitting quality is a critical step in frequency-domain measurements. Evaluation is usually done by nonlinear least squares analysis, seeking to obtain a correlation parameter, χ^2, near unit. Mathematical tools are available providing valuable help, but careful analysis and a lot of experience is necessary for full insight of the data.

6.3.3.5 Techniques and Instrumentation

In addition to all the instrumentation associated to steady-state measurements, frequency-domain spectrofluorometers require a modulated light source and the associated RF electronics. The light source can be an arc lamp followed by a monochromator, in which case the modulation can be achieved by an electro-optic (EO) modulator, usually a Pockels cell. Typically, high driving voltage is required to operate these devices. In addition, careful optimization is needed in these setups because EO modulators have small active areas and work best with collimated light. This way, the excitation optical power obtained with this configuration is usually low. Nevertheless, commercial systems are available using this arrangement, in which arc lamps can be modulated up to 200 MHz. In applications where higher excitation powers are needed, the EO modulators can be used with a variety of *CW* laser sources. These sources, however, are more expensive and cover only limited wavelength ranges. Intrinsic modulated light sources,

like diode lasers and LEDs, can overcome most of these problems. Presently, low-cost LED sources are widely available in the blue-violet range of the spectrum. Although more expensive, some UV LEDs are becoming available. Many frequency-domain sensing applications for chemical species have been reported where low-cost LEDs were used as the light source (McDonagh et al. 2001).

In order to perform measurements of phase angles and modulation at such high frequencies, special techniques must be used. Presently, most frequency-domain instruments are based on a multifrequency cross-correlation detection technique (MFCC). This technique requires that the gain of the PMT should be modulated at the same frequency as the excitation beam, f_m, plus a small frequency offset Δf, that is, at a frequency $f_m + \Delta f$. With adequate electronic filtering, this system yields a signal at the difference frequency, Δf, usually in the 100–1000 Hz range, that contains the same phase and modulation information as the original high-frequency signal. This way, all the measurements can be performed in a low frequency range, using a zero-crossing detector and a ratio digital voltmeter, independently of the modulation frequency. With this method, high-frequency harmonics and other sources of noise are rejected, allowing measurements at lower frequencies to be performed with high accuracy. For instruments using a *CW* laser, the standard deviations of 0.1–0.2° for the phase shift and 0.002–0.004 for the modulation ratio can be obtained.

Similar to time-domain techniques, detectors with short impulse responses are also needed in frequency-domain measurements, in order to avoid signal demodulation due to the instrumentation. The necessary bandwidth will depend on the lifetimes to be measured. For a given luminophore, the frequency range of interest is approximately given by $\omega = 1/\tau$. Typically, for luminophores with lifetimes around 10 ns, modulation frequencies in the 2–200 MHz are adequate. Picosecond lifetimes, on the other hand, will require modulations in the GHz range. Due to their fast responses, PMTs and MCT PMTs are also widely used in frequency-domain spectrofluorometers. The gain of regular PMTs can be easily modulated by injection of the RF signal in one of its dynodes. Typical bandwidths are in the 200–300 MHz range. With MCT PMTs, much higher bandwidths can be achieved (2–5 GHz) with these devices; however, cross correlation must be performed using an external circuit. Although they are seldom used in laboratorial instrumentation because of limited gain, photodiodes, in combination with lock-in amplifiers, are being increasingly used for frequency-domain measurements particularly in sensing application based in long-lived luminophores.

Frequency-domain spectrofluorometers usually have two detectors, one for the sample and one to serve as a reference. The reference PMT usually measures part of reflected or scattered excitation light. On the other hand, the sample detector is alternatively exposed to luminescence from the sample or to excitation light from a scattering solution. This way, performing a relative measurement the arbitrary phase angles due to delays in cables and electronic circuits can be eliminated and an absolute phase shift and modulation ratio, accounting only for the luminophore lifetime, can be retrieved. Although this referencing technique allows compensating for the influence of many external parameters, some problems common to time-domain devices may still be observed, such has wavelength dependence of detector sensitivity and polarization effects.

Presently, from the instrumental point of view, laboratorial devices for time-domain and frequency-domain measurements are very similar in cost and performance. Nevertheless, differences exist that may be important in specific applications. For the

particular case of low-cost sensing applications, frequency-domain measurements present some considerable advantages. Frequency-domain measurements are usually faster; the sinusoidal signals are easier to measure than the very short decay signals characteristic of time-domain measurements; no deconvolution is necessary, saving computation time and money in complex analyses software. Overall, considering specific applications, frequency-domain systems can usually be implemented with simpler electronics and at lower cost than time-domain systems. Nevertheless, luminescent emission can sometimes be too weak for frequency-domain detection, where signal must be strong enough to make zero-crossing detection. In these cases, time-domain SPT with longer acquisition times are extremely sensitive and can still be used.

6.4 Fluorescent Sensing and Imaging

Sensing and imaging applications based in luminescence can be extremely sensitive. Unlike absorption where measurements are performed comparing two light intensities that, sometimes, differ less than 1%, luminescence measurements are performed against a dark background. This way, signal-to-noise ratios in luminescence can be very high, even when faint signals are being measured. In certain conditions, even the luminescence of a single molecule can be measured. Luminescence, on the other hand, can be very sensitive to the external medium. This way, it is the perfect probe to perform a wide variety of measurements.

One of the most attractive features of fluorescence-based techniques lie in the possibility of using fluorescent molecules, called probes or indicators, to study nonfluorescent species. While a great deal of molecules can display intrinsic fluorescent emission, more often than not, a fluorescent probe must be used to label the target analyte. Indeed, fluorescent labeling allows targeting particular components with exquisite sensitivity and selectivity enabling trace detection of analytes or imaging of complex biomolecular assemblies, such as living cells.

6.4.1 Fluorescent Indicators

The luminescent probe or indicator is one of the most critical components in any luminescence-based sensing or imaging system. Ultimately, the photophysical and photochemical properties of the sensing dye will determine the characteristics of the whole system. The luminophore absorption and emission spectra will establish the spectral range of the optical source and detector. The modulation frequencies or pulse widths, on the other hand, will be determined by the probe lifetime. In addition, the properties of the dye will determine available sensing mechanisms, with which analytes can be studied. For this reason, a great deal of research has been devoted to the development of luminescent probes with adequate characteristics for a range of applications. This way, in addition to many substances that are naturally luminescent, many other synthesized organic and inorganic compounds are available nowadays.

6.4.1.1 Intrinsic Luminophores and Organic Dyes

A distinction can be made between intrinsic and extrinsic luminescent probes. Intrinsic luminophores are those occurring naturally and include aromatic amino acids, NADH, and chlorophyll, among others. These probes are ideal in the sense that they are already

part of the studied environment, and measurements can be performed with minimum interference. For instance, the presence of tryptophan and tyrosine residues (luminescent amino acids) in proteins is often used to study the shape or the biological function of enzymes. However, such examples are limited, and most of the time, the molecule of interest is nonluminescent and an extrinsic luminescent probe must be introduced.

Most of the naturally occurring luminescent bio-probes have absorption and emission spectra in the UV/blue region of the spectrum. In the particular case of amino acids, absorption usually occurs in the 260–300 nm range and emission spans from 280 to 350 nm. Such energetic radiation can have a harmful effect when studying living systems. In addition, these wavelengths are out of the range of cheaper solid-state sources and detectors and require the use of quartz optics. Moreover, the fast lifetimes usually associated (3–5 ns) require more expensive instrumentation. A particular interesting example of a naturally occurring luminescent probe comes from GFP or green fluorescent protein. Originally isolated from marine organisms, it has been reengineered in different ways to improve its spectral properties (e.g., absorption at 488 nm, coinciding with Argon laser excitation, and emission at 509 nm). As a protein, it could be harmlessly incorporated in different processes of living cells (including genetic expression) revolutionizing the bio-applications of fluorescence microscopy.

Thousands of synthesized luminophores, mostly organic, are now available for the labeling of biological systems or for sensing applications (Wolfbeis 1997, Lakowicz 1999). Usually, they are either covalently bound to the molecule of interest or simply associated to it (by polarity or some other chemical affinity). Most of these dyes have some kind of sensitivity to the environment, through quenching or some other mechanism, enabling their use as sensor of some analyte (pH, ions, oxygen). It is usually desirable that these luminophores have longer absorption and emission wavelength. Primarily, the aim is to avoid interference with or from the intrinsic biological luminescence that can act as background luminescent noise. In addition, it is desirable from the instrumental point of view (sources, detectors, optical fibers transmission properties) to work with visible and near-infrared wavelengths instead. Although this has been accomplished to some extent, nowadays, luminophores are available covering the whole visible spectrum, and some options are even available in the near infrared. Nevertheless still a majority of dyes available require UV or blue excitation.

Although there are exceptions, these properties are common to most organic luminophores. In addition, it should be considered that each of these dyes usually presents different chemical properties. This further complicates their combined use and demands for the development of dedicated protocols for synthesis, functionalization, and immobilization. Also, most organic dyes present high degree of photodegradation hindering their use in long-term sensing applications. In this context, the advent of a family of long-lived and photostable dyes, with more homogeneous spectral and chemical properties and large Stokes shifts, suitable for the sensing of chemical and biological species is highly desirable. Presently, this gap is being filled by hybrid metallo-organic luminescent complexes.

6.4.1.2 Long-Lived Transition Metal Complexes

Originally developed for solar-energy conversion applications, transition metal complexes (TMCs) are now being extensively explored in a wide range of sensing applications. These complexes are characterized by a transition metal containing one or more

organic ligands (typically diimines). Special attention is being devoted to those complexes with platinum metals (Ru, Os, Re, Rh, and Ir), from which ruthenium is by far the most studied case (Watts and Crosby 1971, Juris et al. 1988, Carraway et al. 1991, Demas and DeGraff 1991, Mills and Williams 1997).

Ruthenium complexes have very desirable features for sensing applications. They are long lived, with lifetimes ranging from 100 ns to 7 μs, making them suitable for simpler and less expensive time-domain and frequency-domain measurements. They present relatively high quantum yields, independent of the excitation wavelength and that can go up to 0.5. Most ruthenium complexes display strong absorption bands in the visible range (around 470 nm), which overlap perfectly with the emission of low-cost blue LEDs. In addition, they present a large Stokes shifts with emission typically occurring around 600 nm. In Figure 6.6, the absorption and emission spectra of the ruthenium dye $Ru(dpp)_3$ having diphenyl-phenanthroline ligands can be seen, alongside with its molecular structure.

In comparison to traditional organic dyes, TMC are photochemically and thermally very stable. Chemically, they are extremely versatile due to the organic ligands. One or more of these ligands can be chemically modified to adjust the net electrical charge of the complex, to provide functional groups in order to attach the dye to a polymer support, to neutralize or enhance the interaction of the dye with a given analyte, or to adjust its spectroscopic properties.

Many of the interesting photophysical and photochemical properties of these complexes derive mostly from their unique electronic states. In ruthenium complexes of interest, the ligands are easily reduced and electrons are promoted from the metal to the ligand. These states are also called metal-to-ligand charge-transfer (MLCT) states and are the most remarkable feature of TMC, being responsible for their absorption bands in the visible range (shown in Figure 6.6).

After a fast and efficient intersystem crossing process, electrons rapidly relax to the MLCT triplet states. Emission from these triplet states is responsible for the characteristic orange-red luminescence associated with ruthenium dyes and is formally classified

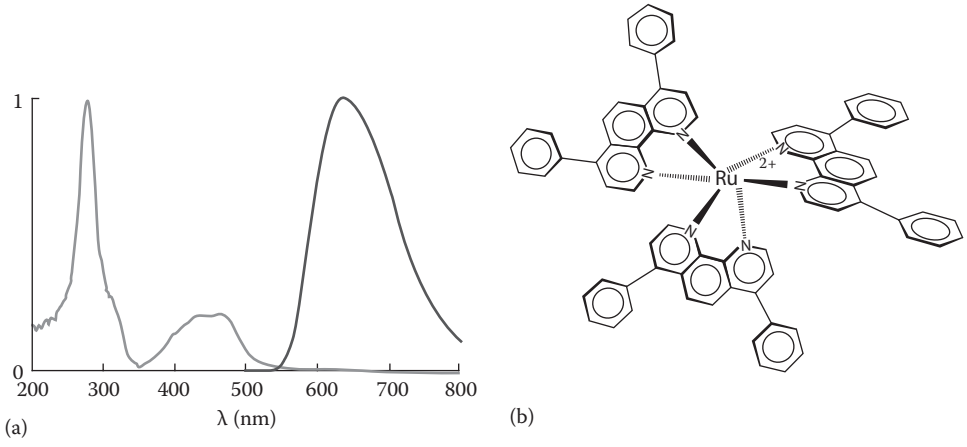

FIGURE 6.6 (a) Absorption (gray trace) and emission (black trace) spectra of the ruthenium complex $Ru(dpp)_3^{2+}$ dissolved in methylene chloride. (b) Dye molecular structure.

as phosphorescence. Nevertheless, the presence of the heavy metallic atom favors spin–orbit coupling, thus resulting in shorter lifetimes (μs) than typical phosphorescent compounds (ms or longer). This way, emission can occur prior to total quenching and these dyes usually display strong luminescence.

Due to their long lifetimes, most ruthenium dyes are very sensitive to collisional quenching by oxygen. The ruthenium complex represented in Figure 6.6 is one the most widely used for oxygen sensing. A long list of applications of these dyes as oxygen sensors has been reported (Carraway et al. 1991, MacCraith et al. 1993, 1994a, McEvoy et al. 1996), including in commercially available products.

In addition to oxygen sensing, the use of complexes with modified ligands has also been reported where the dye luminescence was made sensitive to humidity, pH, or CO_2. Some other examples include applications as quantum counters, DNA probes, study of membranes and proteins, immunoassays, and ion sensing.

These applications demonstrate the possibility of developing a homogeneous set of sensing dyes, with identical photophysical and photochemical properties, based on a single family of coordination compounds (Orellana and Fresnadillo 2004). Although this versatility may raise some concern about cross sensitivities, particularly to oxygen, the combination of the dye with adequate solid membranes can greatly enhance sensor selectivity. This way, conditions are created to the development of a family of chemical sensors, suitable for a wide variety of analytes and with similar enough characteristics to be operated with the same basic instrumentation.

6.4.1.3 Luminescent Quantum Dots

With the advent of nanotechnology, new types of luminescent materials are becoming available having unique properties. Such is the case of QDs or semiconductor nanocrystals. QDs are extremely small particles of semiconductor material, consisting of a few hundreds to a few thousands of atoms. Their small size, ranging from 1 to 20 nm, is mostly responsible for their unique optical, electrical, and chemical properties (Gaponenko 1998). The main differences between the macrocrystalline material and the corresponding nanocrystal arise from two fundamental factors that are size related. The first is associated with the large surface-to-volume ratio of nanoparticles and the second is related to the 3D quantum confinement of their charge carriers. When reduced to the nanometer scale, the size of the particle starts to interfere with its electronic distribution. To a first approximation, it can be shown that a QD behaves as an atomic-like structure with the following energy level distribution:

$$E_{nl} = E_g + \frac{\hbar^2}{2\mu a^2}\chi_{nl}^2 \tag{6.15}$$

where

E_g is the band gap energy of the corresponding bulk semiconductor
a is the QD size

This shows that, in a QD, the band gap is increased by an amount inversely proportional to the size of the nanoparticle. Therefore, the smaller the particle, the higher is its emission energy. This way, it becomes possible to tune the emission wavelength

of nanoparticles by simple control of its size. Bright and relatively narrow emission spectrum, wide range absorption, and extremely high photostability are some of the other features offered by QDs.

Like bulk semiconductor materials, nanocrystal QDs will absorb any wavelength to the blue of their emission peak, that is, any photon with energy higher than that of the lowest transition is absorbed. Moreover, the probability of absorption grows with increasing photon energy, as more and more transitions with higher energy become possible. The very broad absorption spectrum observed in real QDs is a major feature when compared with organic dyes whose absorptions are relatively narrow and in the vicinity of their emission (small Stokes shift). This means that QDs can be excited by any wavelength lower than its emission peak and, unlike dyes, several different kinds of QDs can be simultaneously excited by the same optical source.

Akin to semiconductor, QDs display a relatively narrow emission spectrum. The major source of emission broadening in QDs, however, comes from their size distribution. In a colloidal dispersion, the solid particles have approximately, but not exactly, the same size resulting in slight variations in the emission wavelength. As a consequence, the emission spectrum of a certain ensemble of nanocrystals will be much broader than the individual QDs spectra. Presently, size distributions with less than 5% variation are achievable. This translates into an FWHM of approximately 25 nm, which is quite narrow in comparison to many luminescent dyes. This way, in contrast with traditional dyes, which have broad emission spectra with a characteristic long red tail, nanocrystals present a symmetrical and relatively narrow emission.

The picture in Figure 6.7 was taken with no filters and shows the very distinct emissions of CdTe QDs of different sizes, simultaneously excited using a single blue laser (475 nm).

Most popular methods to produce semiconductor nanoparticles are based in colloidal chemistry where, by a series of engineered reactions using adequate precursors,

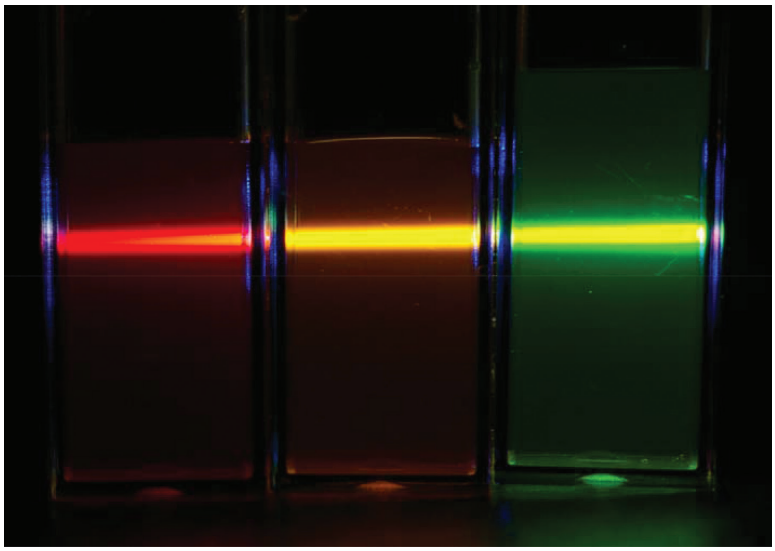

FIGURE 6.7 CdTe QDs with different sizes excited by a single blue laser (475 nm) showing emission at 620, 580, and 540 nm.

Table 6.2 Luminescence Emission Range of QDs Made with Different Semiconductor Materials and of Different Sizes

Semiconductor Material	Emission Range (nm)	QD Size Range (nm)
CdSe	465–640	1.9–6.7
CdSe/ZnS	490–620	2.9–6.1
CdTe/CdS	620–680	3.7–4.8
PbS	850–950	2.3–2.9
PbSe	1200–2340	4.5–9

nanoparticles arise by precipitation. Size can be controlled by timely arresting the reaction with passivating agents (Trindade et al. 2001).

There are practical limitations to the size of the particles that can be achieved with a certain material. When the nanocrystals are made progressively bigger, the quantum confinement is eventually lost. On the other hand, they cannot be made infinitely small. This way, any given material provides tunability over a limited wavelength range. In order to cover a wider range of wavelengths, a variety of materials should be used. Table 6.2 shows the semiconductor materials most commonly used to fabricate nanocrystals by chemical methods. The wavelength range and the corresponding particle size covered by each material are also shown. Roughly a wavelength range of 2000 nm is covered with four different materials.

While most dyes present severe photodegradation when illuminated by energetic radiation, QDs have demonstrated to be extremely photostable in most situations. Although photobleaching has been reported in bare dots, nanocrystals with an adequate protective shell of a different semiconductor material, also called core–shell QD, are known to remain extremely bright even after several hour of moderate to high levels of UV radiation exposure (Hines and Sionnest 1996). On the other hand, the luminescence emission of common dyes can vanish completely after few minutes.

The unique properties of QD have been explored in a wide diversity of imaging and sensing applications (Jorge et al. 2007). Besides outperforming dyes in traditional bioassays and imaging applications, QDs also introduced new possibilities. Their unique photostability and potentially low cytotoxicity allow for long-term in vivo imaging (Dubertret et al. 2002, Jain and Stroh 2004, Jaiswal and Simon 2004, Kirchner et al. 2005) and monitoring of dynamic cell processes. Although cadmium ions alone can be highly toxic to cells, coating the core–shell dots with lipid layers minimizes the risk of contamination. Nevertheless, the toxic nature of the materials used in most QD materials is a concern (Hardman 2006). Presently, heavy metal-free QDs are making its appearance along with alternative nontoxic nanomaterials like carbon dots (Silva 2011). Indeed, a diversity of nanoscale materials and devices is being explored, adding a new dimension of control over luminescent properties and enabling new applications of luminescent spectroscopy.

6.4.2 Fluorescence Quenching

In most sensing applications, the luminophore is used as a probe, and the goal is to measure the concentration of some analyte, through the influence it has on the probe. Depending on the combination luminophore–analyte, different detection

schemes can be used. The analyte concentration can impact the luminescent intensity, the lifetime, the spectral characteristics of emission, etc. Conversely, this influence can take place through a variety of interaction mechanisms, namely, resonant energy transfer, photo-induced electron transfer, and proton transfer. Many of these phenomena have been used successfully as sensing mechanisms, each of them with advantages and disadvantages depending on the specific application. The detection of the concentration of an analyte through collisional quenching of luminescence, in which the analyte is usually the quencher, is a particularly successful approach that has been used for the sensing of many chemical and biological analytes (Geddes 2001).

This technique is often compatible with either intensity or lifetime detection. Furthermore, several models are available, describing different quenching mechanisms that provide simple calibration functions. The term quenching refers, broadly, to any decrease in the luminescence intensity due to the presence of an external agent. Depending on the deactivation mechanism, the excited state lifetime of the luminophore is often decreased as well. Quenching is a bimolecular process involving the interaction between an excited luminescent molecule and the external quencher molecule, *Q*. The result of this interaction is the nonradiative deactivation of the luminophore. This can be achieved by a variety of mechanisms such as electron transfer, proton transfer, energy transfer, molecular rearrangements, or even formation of new molecular compounds (Eftink 1991, Valeur 2002).

6.4.2.1 Dynamic Quenching

A great deal of quenching mechanisms are photophysical processes meaning that, after all the de-excitation steps, the luminophore gets back into the ground state unaltered. These are reversible dynamic quenching processes in which a reduction in the quencher concentration results in an increase of the luminescent signal. The presence of a quenching agent, in a given concentration, introduces an additional external nonradiative decay rate in the luminescence process. As a consequence of the competition between intermolecular processes and the intrinsic deactivation mechanisms, both the quantum yield and the lifetime of luminescence can be decreased. Dynamic quenching processes usually follow a Stern–Volmer (SV) kinetics (Lakowicz 1999):

$$\frac{\tau_0}{\tau} = 1 + K_{SV}[Q] \tag{6.16}$$

where $K_{SV} = k_q \tau_0$ is the SV constant, which depends on the intrinsic lifetime, τ_0, and on the rate constant of the luminophore–quencher interaction k_q. This relation provides a way to monitor the concentration of a given quencher by comparing the quenched lifetime, τ, with the lifetime in the absence of the quencher, τ_0. A similar SV relation can be obtained for the luminescence intensities as well:

$$\frac{I_0}{I} = 1 + K_{SV}[Q] \tag{6.17}$$

where I and I_0 represent the steady-state luminescence intensities (obtained for a given pair of excitation and emission wavelengths). Comparing Equations 6.16 and 6.17, it is found that

$$\frac{I_0}{I} = \frac{\tau_0}{\tau} \tag{6.18}$$

This is a very distinct characteristic of purely dynamic quenching processes where, in the presence of the quencher, both the lifetime and the luminescence intensity are reduced. The decrease in the lifetime occurs because the quencher introduces an additional decay rate that depopulates the excited state. Because the deactivation process is nonradiative, the quantum yield is decreased as well. That is not the case of static quenching where usually chemical reactions are involved that change the ground state population instead. Therefore, only the luminescence intensity is decreased, whereas the lifetime remains constant.

Quenching data are usually obtained in the form of an SV plot where I_0/I or τ_0/τ is represented as a function of quencher concentration, [Q]. If only purely dynamic quenching is present, a linear behavior will be observed as described by Equations 6.17 and 6.18. Overall, the observation of a linear variation in the SV plot is a good indication that a single class of luminophore, homogeneously distributed and with equal access to the quencher, is present in the solution. In rigid media, however, it is often the case that different environments are created in which the quencher has different accessibility. In such situation, the observed SV plot departs from linearity presenting a downward curvature. Transient phenomena arising at high concentration, temperature, viscosity, and other sample conditions can also distort the SV behavior. For many of these cases, however, modified SV models can be used that account for these modification and allow for correct data interpretation.

For the particular case of sensing applications, however, data analysis can be greatly simplified. Most of the time, the quencher is the analyte under study and the goal is simply to determine its concentration. In this context, the simplest quenching models can still be used, and the choice should be made based on the fitting quality. The sensing of chemical species by luminescence quenching techniques has been used successfully in many applications, where very simple models were used, but still taking advantage of the very high sensitivity that is intrinsic to luminescence techniques (MacCraith et al. 1993, Chuang and Arnold 1998, Geddes 2001, Zhoua et al. 2004).

Examples of collisional quenchers include oxygen, amines, halogens, and acrylamide. The actual quenching mechanism can vary with luminophore–quencher pair. For instance, while acrylamide quenches indole by electron transfer processes, quenching by halogens is usually due to spin–orbit coupling inducing intersystem crossing to triplet states. Oxygen is an efficient collisional quencher of almost all known luminophores and it has often to be removed from solutions in order for other quenching processes to be studied. On the other hand, the quenching of luminescence is a preferred method for the optical detection of oxygen and is in the base of some pioneer application of solid-state optrodes.

6.4.3 Fluorescent Optrodes

Luminescence-based techniques are very powerful tools frequently used in a range of applications, from material characterization to the study of molecular dynamics. Although very sensitive and versatile, luminescent methods are usually associated with very complex and expensive instrumentation and, therefore, its use was for long restricted to research laboratories. In the last 20 years, however, revolutionary developments in many different areas have concurred to change this picture (Kulmala and Suomi 2003). The developments in optoelectronics, with the advent of solid-state optical sources including the blue range of the spectrum, together with contributions from organic chemistry, with the creation of long-lived, photostable, metallo-organic luminescent complexes, have made possible the implementation of highly sensitive frequency-domain techniques in low-cost sensing applications (Demas and DeGraff 1997, Juris 1988, Wolfbeis et al. 1998). Great advances in material sciences contributed to the development of sophisticated immobilization techniques, with polymer and solgel chemistry, allowing the design of solid-state luminescent sensors (MacCraith et al. 1995, Mohr 2004, Podbielska et al. 2004). All these advances have made possible to associate the potentialities of luminescence-based techniques with the intrinsic capability of optical waveguides like fibers or integrated optics platforms. Presently, luminescence-based optrodes are being widely explored in the design of chemical sensing probes and lab-on-a-chip platforms, with commercial systems already in the market (Mignani and Baldini 1996, Holst and Mizaikoff 2002).

6.4.3.1 Membranes for Optical Chemical Sensing

One of the most critical steps for the implementation of a solid-state luminescent optrode is the immobilization of the luminescent indicator in a solid matrix. In order to fabricate a sensing probe capable of continuous measurement, the indicator chemistry must be immobilized over the waveguide. This is usually done by encapsulating the luminophores in a solid host. The resulting sensing membrane can either be directly bound to the fiber surface, in an intrinsic approach, or attached to it by some physical support in an extrinsic configuration. Ultimately, the properties of the sensing membranes will determine the sensor performance (Draxler et al. 1995, Demas and DeGraff 1999, Rowe et al. 2002). An ideal immobilization membrane would effectively entrap the indicator and preserve its optical and chemical properties, avoiding leaching and photobleaching. Simultaneously, it should allow the establishment of a fast and reversible equilibrium with the aqueous environment or gaseous atmosphere being probed. While permeability to the analyte is a highly desirable feature, penetration of potentially interfering chemical species into the sensing membrane should be avoided. On top of these requirements, a good adhesion to the waveguide surface, together with mechanical and chemical stability, is a particularly important feature for long-term practical applications.

The simultaneous fulfillment of all these requirements is extremely difficult to obtain, especially considering that every analyte–luminophore combination may have specific chemical properties. Traditionally, polymers are materials of choice for this task due to their chemical versatility and availability in a great variety (Mohr 2004). Although many successful sensing applications using polymers doped with luminescent indicators have

been reported, the sensing membranes are far from ideal and some problems subsist. Major issues are the leaching of the sensor from the solid host, poor chemical resistance, and modification of the properties of the sensing dye.

In this context, solgel glasses are a particular kind of polymeric material having very suitable properties for sensing applications (Podbielska et al. 2004). With this technique, porous silica matrices can be formed that are highly compatible with silica fibers and waveguides. In addition, the sensing dye is physically encapsulated in the microporous structure, avoiding leaching while preserving the indicator chemical properties.

Solgel-derived materials, particularly those based in silica alkoxide precursors, have been attracting the attention of many researchers working in the immobilization of sensing luminophores in solid supports. In comparison to some polymers, these materials can be mechanically robust and chemically very resistant. In addition, by choosing the right ingredients and adjusting the process parameters, properties like polarity and porosity can be tailored to the specific needs of an application (Hench and West 1990, McDonagh et al. 1998). Furthermore, they are usually optically transparent, and their refractive index can be tuned within a wide range. The simplicity and low temperatures associated to the fabrication process, along with the compatibility with a variety of coating processes (spin coating, dip coating, casting, spraying), make them suitable for use in either very specific laboratorial applications or in large-scale industrial processes. High-quality thin-film layers where the luminescent dye preserves its sensing properties can be obtained using the solgel process. Shown in Figure 6.8 is a circular glass substrate spin coated with a thin solgel film (thickness around 1 μm) doped with an oxygen-sensitive luminescent ruthenium complex. The thin-film layers are excited by a LED source (475 nm) through a large-diameter fiber bundle at the center of the substrate, where an intense luminescent spot can be observed.

In addition, high brightness luminescence is also observed coming out of the substrate edges. This happens because part of the isotropic fluorescent emission is trapped inside the glass substrate being guided toward its edged by a waveguide effect. Taking advantage of such effects, it is possible to design highly efficient luminescent optrodes

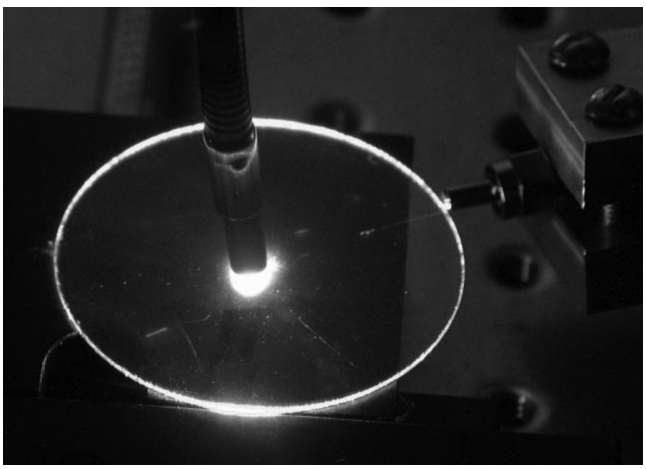

FIGURE 6.8 Thin film doped with 10 mM Ru(bpy) displaying strong luminescence when excited with a blue LED.

using planar waveguides or optical fibers. Indeed, solgel layers and ruthenium-based complexes are in the base of some of the most successful applications of luminescent-based optrodes for chemical sensing (Jorge et al. 2004).

6.4.3.2 Fiber-Optic Luminescent Optrodes

A wide variety of luminescent optrodes where a luminescent indicator is immobilized in a solid substrate and used as sensing probe, either in planar or in fiber-optic platforms, have been reported to date. Optical fiber-based optrodes, in particular, have made possible the use of conventional spectroscopy techniques in sites otherwise inaccessible. In addition, their unique characteristics have provided new possibilities like multiplexing capability and evanescent wave sensing. These features along with the technological advances in the field of optoelectronics and material science have allowed for the establishment a mature optical fiber biochemical sensing technology. Presently, with many fundamental proof-of-principle sensing schemes already demonstrated, a growing number of practical applications are being explored in a wide range of situations (Wolfbeis 2002, 2004, Narayanaswamy and Wolfbeis 2004). Major areas currently explored include medical and chemical analysis, molecular biotechnology, marine and environmental analysis, and bioprocess control.

One of the most popular and successful applications of the use of fiber-optic luminescent optrodes is the optical detection of oxygen by luminescence quenching. Its history is representative of the state of the art of luminescent optrode technology.

Although fiber optics has been used in very early luminescent oxygen sensing applications, the fiber was typically used simply as a light-guiding device through which excitation and detection of radiation were performed. Only after the development of polymer and solgel immobilization membranes could the first true optical fiber sensing probes be implemented. One of the first reports of a truly intrinsic oxygen fiber probe was made by MacCraith et al. (1994b). The authors used an evanescent wave configuration, where a solgel thin film, doped with Ru(dpp), was deposited over a fiber section with previously removed cladding.

Improvement of the encapsulation chemistry of solgel, using hybrid organic–inorganic materials, enabled to tailor the sensor properties improving sensitivity and photostability. Figure 6.9 shows a representative example fiber-optic luminescent optrode displaying two tapered multimode optical fibers coated with a hybrid solgel material, doped with an oxygen-sensitive ruthenium complex. Tapering is a commonly used technique to improve luminescent coupling efficiency and also to improve the probe spatial resolution (Jorge et al. 2004). In a pioneer work, tapered fibers were used to implement micro-optrodes with fiber tip diameters ranging from 10 to 50 μm (Klimant et al. 1999). The small dimensions of the sensing tip allowed measurements with very high spatial resolution and very fast response times (250 ms). Oxygen gradients with a spatial resolution of up to 20 μm were measured in freshwater sediments covered with a 2 mm layer of green algae.

The luminescence emission of most sensing dyes is generally temperature dependent. This way, most luminescent sensors (and also optical oxygen sensors) need to be provided with a temperature reference. Techniques explored to simultaneously measure oxygen and temperature included the combination of the oxygen-sensitive dye and a phosphorescent crystal (Liao et al. 1997). Alternatively, the use of QDs encapsulated

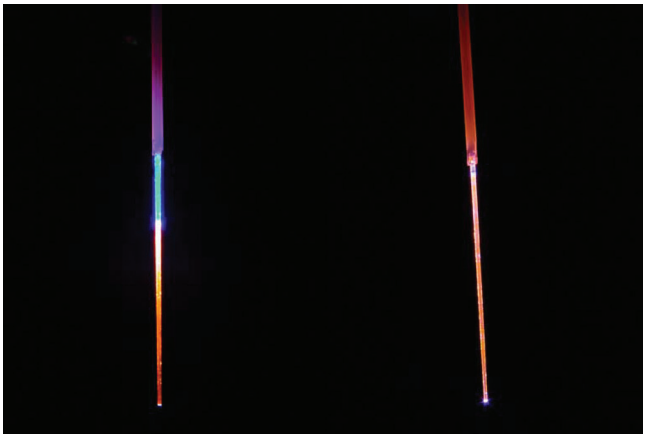

FIGURE 6.9 Picture of tapered fibers coated with solgel thin film doped with an oxygen-sensitive ruthenium complex and excited by a blue LED.

in polymer with low oxygen permeability and therefore sensitive only to temperature was combined with oxygen-sensitive ruthenium complex in a highly permeable solgel matrix (Jorge et al. 2008).

A diversity of practical applications made use of fiber-optic oxygen-sensitive optrodes. A prototype of a multiparameter sensing probe (pH, CO_2, and O_2) using a different fiber for each indicator dye and employed in intravascular monitoring was described (Mignani and Baldini 1996). A high-performance dissolved oxygen optical sensor based on phase detection using an external membrane configuration was developed for application in wastewater monitoring. A detection limit of <10 ppb was achieved and the long-term stability reached several months. In addition, the disposable sensing membrane could be easily substituted (McDonagh et al. 2001).

Many other similar applications were described with sensing optrodes being developed for special conditions. Oxygen measurements could be performed at high temperature, in hyperbaric chambers; sensing heads withstanding sterilization were developed; measurements could be performed in high-pressure fermentation reactors; and several in vitro and in vivo tests were demonstrated successfully (Wolfbeis et al. 1998, Remillard et al. 1999, Stokes and Somero 1999, Zhao et al. 1999).

Presently, a few companies offer a diversity of oxygen sensing probes. Ocean Optics offers a modular system where different kinds of fiber probes, a pulsed blue LED optical source, and a preconfigured CCD spectrometer with dedicated software can be acquired separately. PreSense is a German company offering similar oxygen sensing probes where time-resolved measurements are used instead. In addition to standard probes, micro-optrodes with 30 μm fiber tips are also available, which are suitable for performing high-spatial-resolution measurements of biological samples. A support unit capable of simultaneous interrogation of several sensors allows multipoint measurements to be implemented.

Other companies can be found that offer probes optimized for applications in wastewater treatment or oceanographic applications. Although not advertised, several companies selling oxygen sensors based on conventional technologies are making strong

efforts to introduce optical technologies in their products and maintain close contact with the scientific community.

6.5 Conclusions and Future Outlook

A source of curiosity and fascination in earlier times, photoluminescence is presently the base for some of the most sensitive analytical techniques available and a reference method in many fields of science and industry.

Instrumentation for steady-state and time-domain spectroscopy has experienced dramatic evolution in the last decades, progressing from classical benchtop instruments to a diversity of analytical tools: powerful fluorescence microscopes enable visualization of the internal structure of cells unraveling the mysteries of life; unprecedented sensitivity supports single molecule analysis; fluorescent arrays facilitate fast DNA sequencing; fluorescent immunoassays are the base for some of the most selective biosensors.

Miniaturization, in particular, made possible by the fast progress of optoelectronics (sources and detectors) is taking fluorescence out of the lab into the world of field applications enabling in situ environmental monitoring. The combination of luminescent probes, immobilized in solid-state membranes, into guided wave platforms like optical fibers is the base for a new family of (bio)chemical sensing optrodes with remarkable features and potential of application (environmental monitoring, bioprocess control, single cell analysis, operation in chemically and electromagnetically hazard environments).

Presently, a new revolution is happening with the advent of nanotechnology. Control at the nanometer scale, combining different materials in different geometries, allows tailoring the optical, chemical, and mechanical properties of materials. New luminescent probes like QDs, with very high photostability, are enabling unprecedented applications like long-term in vivo cellular imaging that are literally shedding new light into biochemistry.

In the near future, combination with metamaterials made from the merging of different nanostructures like metallic nanopillars or graphene will allow unparalleled control over the properties of light pushing forward the possibilities of photoluminescence.

References

Carraway, E.R., Demas, J.N., DeGraff, B.A., and Bacon, J.R., Photophysics and photochemistry of oxygen sensors based on luminescent transition-metal complexes. *Analytical Chemistry*, 1991. 63: 337–342.

Chuang, H. and Arnold, M.A., Linear calibration function for optical oxygen sensors based on quenching of ruthenium fluorescence. *Analytica Chimica Acta*, 1998. 368: 83–89.

Demas, J.N., DeGraff, B.A., and Coleman, P.B., Oxygen sensors based on luminescence quenching. *Analytical Chemistry* 1999. A793–A800.

Demas, J.N. and DeGraff, B.A., Design and applications of highly luminescent transition metal complexes. *Analytical Chemistry*, 1991. 63: 829A–837A.

Demas, J.N. and DeGraff, B.A., Applications of luminescent transition metal complexes to sensor technology and molecular probes. *Journal of Chemical Education*, 1997. 74: 690–695.

Draxler, S., Lippitsch, M.E., Klimant, I., Kraus, H., and Wolfbeis, O.S., Effects of polymer matrices on the time-resolved luminescence of a ruthenium complex quenched by oxygen. *Journal of Physical Chemistry*, 1995. 195: 3162–3167.

Dubertret, B., Skourides, P., Norris, D.J., Noireaux, V., Brivanlou, A.H., and Libchaber, A., In vivo imaging of quantum dots encapsulated in phospholipid micelles. *Science*, 2002. 298: 1759–1762.

Eftink, M.R., Fluorescence quenching: Theory and applications, in *Topics in Fluorescence Spectroscopy: Principles*, J.R. Lakowicz, ed. 1991, New York: Plenum Press. pp. 53–120.

Gaponenko, S.V., *Optical Properties of Semiconductor Nanocrystals*. Cambridge Studies in Modern Optics, P.L. Knight and A. Miller, eds., Vol. 23. 1998, Cambridge, U.K.: Cambridge University Press.

Geddes, C.D., Optical halide sensing using fluorescence quenching: Theory, simulations and applications—A review. *Measurement Science and Technology*, 2001. 12: R33–R88.

Hardman, R.A., Toxicologic review of quantum dots: Toxicity depends on physicochemical and environmental factors. *Environmental Health Perspectives*, February 2006. 114(2): 165–172.

Hench, L.L. and West, J.K., The sol-gel process. *Chemical Reviews*, 1990. 90: 33–72.

Hines, M.A. and Sionnest, P.G., Synthesis and characterization of strongly luminescing ZnS-capped CdSe nanocrystals. *Journal of Physical Chemistry*, 1996. 100: 468–471.

Holst, G. and Mizaikoff, B., Fiber optic sensors for environmental applications, in *Handbook of Optical Fibre Sensing Technology*. 2002, Lôpez-Higuera, J.M. (Ed.), New York: John Wiley & Sons, Ltd. pp. 729–755.

Jain, R.K. and Stroh, M., Zooming in and out with quantum dots. *Nature Biotechnology*, 2004. 22(8): 959–960.

Jaiswal, J.K. and Simon, S.M., Potentials and pitfalls of fluorescent quantum dots for biological imaging. *Trends in Cell Biology*, 2004. 14(9): 497–504.

Jorge, P.A.S., Caldas, P., Rosa, C.C., Oliva, A.G., and Santos, J.L., Optical fiber probes for fluorescence based oxygen sensing. *Sensors and Actuators B—Chemical*, 2004. 103(1–2): 290–299.

Jorge, P.A.S., Martins, M.A., Trindade, T., Santos, J.L., and Farahi, F. Optical fiber sensing using quantum dots. *Sensors*, 2007. 7(12): 3489–3534.

Jorge, P.A.S., Maule, C., Silva, A.J., Benrashid, R., Santos, J.L., and Farahi, F., Dual sensing of oxygen and temperature using quantum dots and a ruthenium complex. *Analytica Chimica Acta*, 2008. 606(2): 223–229.

Juris, A., Balzani, V., Barigalletti, F., Campagna, S., Belser, P., and Zelewsky A., Ru(II) polypyridine complexes: Photophysics, photochemistry, electrochemistry, and chemiluminescence. *Coordination Chemistry Reviews*, 1988. 84: 85–277.

Kirchner, C., Liedl, T., Kudera, S., Pellegrino, T., Javier, A.M., Gaub, H.E., Stolzle, S., Fertig, N., and Parak, W.J., Cytotoxicity of colloidal CdSe and CdSe/ZnS nanoparticles. *Nano Letters*, 2005. 5(2): 331–338.

Klimant, I., Ruckruh, F., Liebsch, G., Stangelmayer, A., and Wolfbeis, O.S., Fast response oxygen microoptrodes based on novel soluble ormosil glasses. *Mikrochimica Acta*, 1999. 131: 35–46.

Kuhn, H. and Forsterling, H.-D., *Principles of Physical Chemistry*. 2000, New York: John Wiley & Sons.

Kulmala, S. and Suomi, J., Current status of modern analytical luminescence methods. *Analytica Chimica Acta*, 2003. 500: 21–69.

Lakowicz, J.R., Fluorophores, in *Principles of Fluorescence Spectroscopy*. 1999, New York: Kluwer.

Liao, S.-C., Xu, Z., Izatt, J.A., and Alcala, J.R., Real-time frequency domain temperature and oxygen sensor with a single optical fiber. *IEEE Transactions on Biomedical Engineering*, 1997. 44(11): 1114–1121.

MacCraith, B.D., McDonagh, C.M., O'Keeffe, G., Keyes, E.T., Vos, J.V., O'Kelly, B., and McGilp, J.F., Fibre optic oxygen sensor based on fluorescence quenching of evanescent-wave excited ruthenium complexes in sol-gel derived porous coatings. *Analyst*, 1993. 118: 385–388.

MacCraith, B.D., McDonagh, C.M., O'Keeffe, G., McEvoy, A.K., Butler, T., and Sheridan, F.R., Sol-gel coatings for optical chemical sensors and biosensors. *Sensors and Actuators B*, 1995. 29: 51–57.

MacCraith, B.D., O'Keeffe, G., McDonagh, C.M., and McEvoy, A.K., LED-based fibre optic oxygen sensor using sol-gel coating. *Electronics Letters*, 1994a. 30: 888–889.

MacCraith, B.D., O'Keeffe, G., McEvoy, A.K., and McDonagh, C., Development of a LED-based fibre optic oxygen sensor using a sol-gel-derived coating. In Proc. SPIE 2293, Chemical, Biochemical, and Environmental Fiber Sensors VI, 110 (October 21, 1994b); doi:10.1117/12.190961.

McDonagh, C., Kolle, C., McEvoy, A.K., Dowlingm, D.L., Cafolla, A.A., Cullen, S.J., and MacCraith, B.D., Phase fluorometric dissolved oxygen sensor. *Sensors and Actuators B*, 2001. 74: 124–130.

McDonagh, C.M., MacCraith, B.D., and McEvoy, A.K., Tailoring of sol–gel films for optical sensing of oxygen in gas and aqueous phase. *Analytical Chemistry*, 1998. 70: 45–50.

McEvoy, A.K., McDonagh, C.M., and MacCraith, B.D., Dissolved oxygen sensor based on fluorescence quenching of oxygen-sensitive ruthenium complexes immobilized in sol-gel-derived porous silica coatings. *Analyst*, 1996. 121: 785–788.

Mignani, A.G. and Baldini, F., Biomedical sensors using optical fibres. *Reports on Progress in Physics*, 1996. 59(1): 1–28.

Mills, A. and Williams, F.C., Chemical influences on the luminescence of ruthenium diimine complexes and its response to oxygen. *Thin Solid Films*, 1997. 306: 163–170.
Mohr, G.J., Polymers for optical sensors, in *Optical Chemical Sensors*, F. Baldini et al., eds. 2004, Dordrecht, the Netherlands: Springer. pp. 297–321.
Narayanaswamy, R. and Wolfbeis, O.S., eds. *Optical Sensors—Industrial Environmental and Diagnostic Applications*. Springer Series on Chemical Sensors and Biosensors, O.S. Wolfbeis, ed. 2004, Berlin, Germany: Springer.
Orellana, G., Luminescent optical sensors. *Analytical and Bioanalytical Chemistry*, 2004. 379: 344–346.
Orellana, G. and Fresnadillo, D.G., Environmental and industrial optosensing with tailored luminescent Ru(II) polypyridyl complexes, in *Optical Sensors—Industrial Environmental and Diagnostic Applications*, R. Narayanaswamy and O.S. Wolfbeis, eds. 2004, Berlin, Germany: Springer. pp. 309–357.
Podbielska, H., Ulatowska-Jarza, A., Muler, G., and Eichler, H.J., Sol-gels for optical sensors, in *Optical Chemical Sensors*, F. Baldini et al., eds. 2004, Dordrecht, the Netherlands: Springer. pp. 353–385.
Remillard, J.T., Jones, J.R., Poindexter, B.D., Narula, C.K., and Weber, W.H., Demonstration of a high-temperature fiber-optic gas sensor made with a sol-gel process to incorporate a fluorescent indicator. *Applied Optics*, 1999. 38(25): 5306–5309.
Rowe, H.M., Xu, W., Demas, J.N., and DeGraff, B.A., Metal ion sensors based on a luminescent ruthenium(II) complex: The role of polymer support in sensing properties. *Applied Spectroscopy*, 2002. 56: 167–173.
Silva, J.G.G.E., Carbon and silicon fluorescent nanomaterials, in *Nanomaterials*, Prof. Mohammed Rahman, ed. 2011, Rijeka, Croatia: InTech. pp. 237–252. DOI: 10.5772/25809. Available from: http://www.intechopen.com/books/nanomaterials/carbon-and-silicon-fluorescent-nanomaterials.
Stokes, M.D. and Somero, G.N., An optical oxygen sensor and reaction vessel for high-pressure applications. *Limnology and Oceanography*, 1999. 44(1): 189–195.
Trindade, T., O'Brien, P., and Pickett, N. L., Nanocrystalline semiconductors: synthesis, properties, and perspectives. *Chemistry of Materials*, 2001. 13(11): 3843–3858.
Valeur, B., *Molecular Fluorescence: Principles and Applications*. 2002, Weinheim, Germany: Wiley VCH.
Watts, R.J. and Crosby, G.A., Spectroscopic characterization of complexes of ruthenium(II) and iridium(III) with 4,4'-diphenyl-2,2'-bipyridine and 4,7-diphenyl-1,10-phenanthroline. *Journal of the American Chemical Society*, 1971. 93: 3184–3188.
Wolfbeis, O.S., Chemical sensing using indicator dyes, in *Optical Fiber Sensors: Applications, Analysis and Future Trends*. Dakin, J. and Culshaw, B. (Eds.) 1997, Boston, MA: Artech House. pp. 53–107.
Wolfbeis, O.S., Fiber optic chemical sensors and biosensors. *Analytical Chemistry*, 2002. 72: 81R–89R.
Wolfbeis, O.S., Fiber optic chemical sensors and biosensors. *Analytical Chemistry*, 2004. 76: 3269–3284.
Wolfbeis, O.S., Klimant, I., Werner, T., Huber, C., Kosch, U., Krause, C., Neurauter, G., and Durkop, A., Set of luminescence decay time based chemical sensors for clinical applications. *Sensors and Actuators B*, 1998. 51: 17–24.
Zhang, Z., Grattan, K.T.V., and Palmer, A.W., Phase-locked detection of fluorescence lifetime. *Review of Scientific Instruments*, 1993. 64: 2531–2540.
Zhao, Y.D., Richman, A., Storey, C., Radford, N.B., and Pantano, P., In situ fiber-optic oxygen consumption measurements from a working mouse heart. *Analytical Chemistry*, 1999. 71(17): 3887–3893.
Zhoua, L.L., Suna, H., Zhang, X.H., and Wu, S.K., An effective fluorescent chemosensor for the detection of copper(II). *Spectrochimica Acta Part A*, 2004. 61: 61–65.